Endosomal recycling controls plasma membrane area during mitosis

Emmanuel Boucrot and Tomas Kirchhausen*

Department of Cell Biology and CBR Institute for Biomedical Research, Harvard Medical School, 200 Longwood Avenue, Boston, MA 02115

Communicated by Marc W. Kirschner, Harvard Medical School, Boston, MA, March 16, 2007 (received for review November 21, 2006)

The shape and total surface of a cell and its daughters change during mitosis. Many cells round up during prophase and metaphase and reacquire their extended and flattened shape during cytokinesis. How does the total area of plasma membrane change to accommodate these morphological changes and by what mechanism is control of total membrane area achieved? Using single-cell imaging methods, we have found that the amount of plasma membrane in attached cells in culture decreases at the beginning of mitosis and recovers rapidly by the end. Clathrin-based endocytosis is normal throughout all phases of cell division, whereas recycling of internalized membranes back to the cell surface slows considerably during the rounding up period and resumes at the time at which recovery of cell membrane begins. Interference with either one of these processes by genetic or chemical means impairs cell division. The total cell-membrane area recovers even in the absence of a functional Golgi apparatus, which would be needed for export of newly synthesized membrane lipids and proteins. We propose a mechanism by which modulation of endosomal recycling controls cell area and surface expression of membrane-bound proteins during cell division.

clathrin | endocytosis | exocytosis | cell division | dynasore

A characteristic of eukaryotic cells, particularly when spread on a substrate and unprotected by a cell wall, is to round up during mitosis, becoming more compact at metaphase and recovering during cytokinesis. By altering its size and shape, the cell presumably acquires a mechanism for modulating spatially segregated signaling pathways as it divides (1) and for ensuring transfer of a similar complement of constituents to the daughter cells. Control of membrane dynamics must therefore be linked to progress through the stages of cell division. Simple geometric considerations argue that transformation from an extended cell interphase to a rounded mitotic cell should be accompanied by a large reduction in cell surface, particularly if the cellular volume remains approximately constant after having doubled during the S to M phase transition (2).

One way to accommodate the apparent change in cell area during mitosis is to maintain the total amount of membrane at the cell surface by allowing formation of extensive folds. Imaging by scanning electron microscopy of the surface of synchronized mastocytoma cells grown in suspension showed an increase in the number of microvilli between G_1 and G_2 and an apparent doubling of the surface area; based on these observations it was proposed (3) that "cytokinesis is a physical unfolding or stretching process" that provides the extra surface required for the two daughter cells. Similar studies done with adherent CHO or BHK21 cells also showed a larger number of microvilli, blebs, and ruffles in mitotic rounded cells than in the completely spread cells in interphase (4, 5). In these early studies, however, it was recognized that rapid membrane redistribution through endocytosis and recycling rather than surface stretching could also account for the changes in cell surface (4).

Another way to accommodate the altered surface-to-volume ratio when cells round up is to regulate membrane traffic between the cell surface and its interior, leading to membrane loss at the onset of mitosis and recovery afterward. Imaging along the cell cycle by electron microscopy of neuroblastoma cells showed the appearance of blebs at the plasma membrane and the accumulation of single-bilayer or multilamellar vesicles close to the blebs (6). Based on these observations, it was proposed that fusion of these structures with the plasma membrane was responsible for a substantial increase in cell surface area particularly at late stages during mitosis. Most recent studies on the role of membrane traffic during cell division have focused on delivery and retrieval of membrane at the cleavage furrow during cytokinesis (for a recent review, see ref. 7). A number of proteins found to be essential for cytokinesis also have established functions in endocytic, exocytic, and recycling pathways. Interpretation of these findings have emphasized the role of exocytic events during the actomyosin-based constriction responsible for cleavage furrow formation and for abscission (separation of the two daughter cells).

A number of observations demonstrate profound changes in membrane traffic during mitosis. The Golgi apparatus disassembles thus preventing constitutive exocytosis along the biosynthetic pathway (8, 9). Moreover, transferrin uptake through the clathrin-based endocytic pathway and fluid-phase uptake both decline sharply during metaphase and anaphase (10–13) and recover during telophase (14).

We have capitalized on newly introduced live-cell imaging approaches to reinvestigate the role of membrane traffic in regulating cell surface area. In particular, we have followed individual cells through different stages of the cell cycle, instead of monitoring bulk properties of synchronized populations of cells. We have monitored changes in total plasma membrane in cells undergoing mitosis, and we have correlated these data with the dynamics of endocytosis and exocytosis during all stages of cell division. Three key observations have emerged from these studies: (*i*) the cell surface area decreases at the onset of mitosis, when the mother cell rounds up, and recovers starting in anaphase, with complete recovery before abscission; (*ii*) endocytosis is normal throughout all phases of cell division; and (*iii*) recycling of internalized membranes back to the cell surface slows considerably during the rounding-up period and reactivates by a concerted fusion of endosomes with the plasma membrane, starting in anaphase. This recovery occurs even under conditions in which the Golgi apparatus has been rendered nonfunctional. We propose a simple mechanism in which modulation of endosomal recycling controls surface area during cell division.

Results

Cells Change Plasma Membrane Area During Mitosis. In preparation for cell division, interphase cells growing on a substrate round up

Author contributions: E.B. and T.K. designed research; E.B. performed research; E.B. analyzed data; and E.B. and T.K. wrote the paper.

The authors declare no conflict of interest.

Abbreviation: VAMP, vesicle associated membrane protein.

*To whom correspondence should be addressed. E-mail: kirchhausen@crystal.harvard.edu.

This article contains supporting information online at www.pnas.org/cgi/content/full/0702511104/DC1.

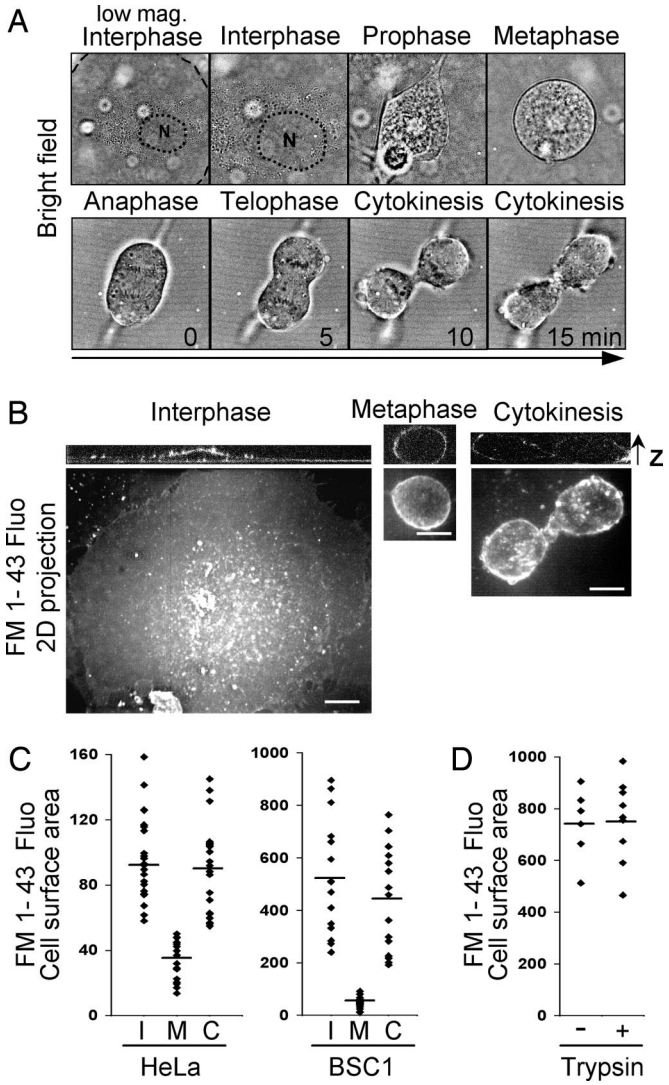

Fig. 1. Changes in cell shape and amount of plasma membrane during mitosis. (*A*) BSC1 cells visualized at several stages during the cell cycle, using bright field. N, nucleus. (*B*) BSC1 cells incubated for 2 min with FM 1-43 dye at 37°C and imaged at the same magnification at interphase, metaphase and cytokinesis. Three-dimensional image stacks were obtained from sequential optical sections acquired 0.25 μm apart by using the spinning disk confocal configuration. Shown is the fluorescence signal along the *z* axis (*Upper*) at its two dimensional projection (*Lower*). The integrated fluorescence, corrected for any fluorescence signal inside the cells, represents the amount of plasma membrane. Scale bar, 10 μm. (*C*) Amount of plasma membrane at different stages during the cell cycle was obtained in six experiments from 45 BSC1 and 64 HeLa cells, respectively. I, interphase; M, metaphase; C, cytokinesis. (*D*) Amount of plasma membrane in BSC1 cells, rounded up immediately after detachment by treatment with trypsin for 5 min at 37°C and then imaged as in *B*. Data from two experiments from nine trypsinized cells and six untreated control cells in interphase and spread on the coverslip.

(Fig. 1*A*), and their surface area, measured as described below, decreases in a process that starts at the onset of prophase and ends with metaphase (Fig. 1*B*). Reversal of these steps begins at anaphase, continues through telophase, and becomes particularly prominent during cytokinesis (Fig. 1 *A–C*). Where does the extra membrane go at the beginning of cell division, and where does it come from at the end? To monitor with high temporal resolution the total plasma-membrane area throughout a complete cell-division cycle, we used three-dimensional, spinning disk confocal, live-cell imaging of single cells labeled with the membrane-impermeant dye, FM 1-43, which becomes fluorescent upon binding to the outer leaflet of the plasma membrane (15) [Fig. 1*B* and supporting information (SI) Fig. 7*A*]. The surface fluorescence signal is a measure of exposed membrane, because the charged head group of FM 1-43 prevents it from flipping to the inner leaflet, and internal membranes can only be reached by endocytic vesicular traffic (15).

Cells selected at different stages during cell division were incubated for a brief time with FM 1-43 at 37°C, and image stacks were acquired after 2 min, a time sufficient to achieve a stable fluorescent signal and short enough to reduce to a minimum the contribution from dye association with endosomal membranes because of endocytosis (Fig. 1*B*, z view). Any remaining intracellular fluorescence was removed from each optical section by manual masking (see *Materials and Methods*). The total surface area within a population of cells at interphase varied widely (Fig. 1*C*). At metaphase, when cells rounded up, we found a large reduction in that area, about two-fold for human HeLa cells and about six- to eight-fold for monkey BSC1 cells (Fig. 1*C*). Nonadherent human Jurkat T cells imaged in the same way display a large amount of plasma-membrane projections during interphase, in stark contrast to the fairly smooth appearance during metaphase (SI Fig. 7*A*), suggesting that the amount of plasma membrane is also lower during metaphase. As a complementary approach to determine cell surface area, we monitored the fluorescence signal at the plasma membrane elicited by a chimera of EGFP fused at its C terminus with the peptide-sorting motif CAAX expressed in BSC1 or HeLa cells (SI Fig. 7 *B* and *C*). We followed the changes in cell surface of single cells and found that it also increases during the transition from metaphase to cytokinesis.

Cell rounding alone cannot account for the observed decrease in surface area, because the surface remained constant in interphase cells that rounded upon brief treatment with trypsin (Fig. 1*D*). That is, the surface of trypsinized cells must ruffle or fold when they round up. In addition, we ruled out a decrease in FM 1-43 dye accessibility during cell rounding by observing that the total amount of intracellular and plasma membrane available (determined by total fluorescence) remained the same in mitotic, trypsinized, or interphase cells when we gently permeabilized their plasma membrane with saponin before incubation with the dye (SI Fig. 8*A*). These data confirm that the decrease of plasma membrane during mitosis is matched by its accumulation inside cells.

The compensatory increase in surface area began at the onset of anaphase and continued throughout cytokinesis, until the two daughter cells had recovered the total area originally present in the mother cell (Fig. 1*C*). Similar results were obtained from sequential measurements of surface area from the same cells imaged at different stages during the cell cycle, using a modified staining protocol (SI Fig. 8*B*). The period of cell membrane reduction lasts 30–45 min, the time it takes cells to round up and reach metaphase. Recovery, which is relatively fast (15–20 min), occurs before a perinuclear Golgi apparatus has assembled (SI Fig. 8*C*).

Endocytosis Is Not Affected During Mitosis. It has been shown by electron microscopy that cells contain plasma membrane coated pits and vesicles regardless of their stage of cell division (16). All endocytic plasma membrane coated pits and vesicles contain clathrin adaptor AP-2 (17). We have now demonstrated that the dynamics of AP-2 incorporation into plasma membrane pits and vesicles during mitosis is the same as in interphase (Fig. 2). We used BSC1 cells stably expressing σ2-EGFP (17), part of AP-2 and imaged the surface attached to the coverslip to facilitate data acquisition (Fig. 2 and SI Movies 1–3). Quantitative analysis of these data (17) shows fluorescent σ2-EGFP spots with equivalent lifetimes during mitosis and interphase (SI Fig. 9 *A*

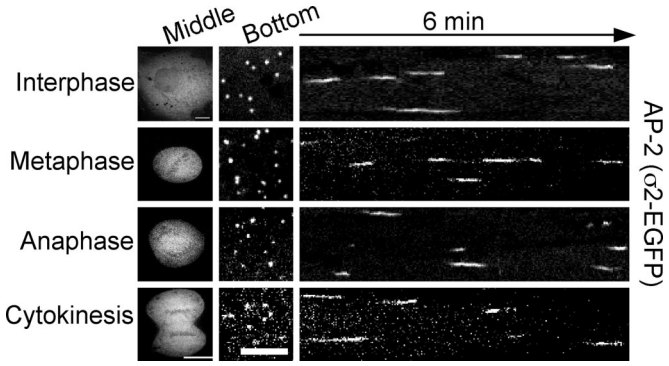

Fig. 2. Formation of clathrin coated pits and coated vesicles is not affected by mitosis. Live cell fluorescence imaging of AP-2, containing clathrin coated pits and coated vesicles located at the bottom surface of BSC1 cells. AP-2 was labeled by stable expression of σ2-adaptin fused to EGFP (17). Time series collected for 6 min and at 37°C from one cell during interphase, and from another cell sequentially imaged during metaphase and anaphase and ≈15 min into cytokinesis. The still images (*Left*) correspond to Middle and Bottom optical sections (scale bars, 10 and 5 μm, respectively) acquired after 3 min of data collection; the kymographs (*Right*) represent the complete time-series. The data are representative of experiments done in triplicate and were acquired every 2 s with 1-s exposures, using the spinning disk confocal configuration.

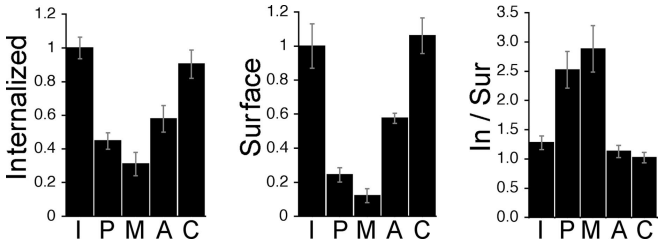

Fig. 3. Receptor-mediated endocytosis of transferrin during cell division. The amounts of internalized transferrin (In) and of transferrin bound to the cell surface (Sur) were obtained by integration of their corresponding fluorescence signals present in the three-dimensional image stacks. The data (mean ± standard deviation) were obtained from 24, 18, 14, 5, and 20 cells imaged at interphase (I), prophase (P), metaphase (M), anaphase (A), and late stages of cytokinesis (C), respectively.

and *B Left*). Thus, the time needed to form a coated pit and for it to bud as a coated vesicle is uniform throughout the cell cycle. In addition, we could detect no change in the sizes of the coated vesicles (SI Fig. 9*B Right*) or in the frequency of assembly events per unit surface area (SI Fig. 9*C*). Similar results were obtained with HeLa cells (SI Movie 4). These observations suggest that endocytosis carried by the clathrin pathway remains normal during mitosis.

Other forms of uptake probably also remain active during mitosis, as the uptake of Alexa-594 labeled (10 kDa) dextran by fluid phase endocytosis continued during mitosis (SI Fig. 10 *A* and *B* for BSC1 cells and SI Fig. 10*C* for HeLa cells). As expected, the internal membranes of rounding cells became labeled by plasma membrane uptake when incubated steadily with FM 1-43 during prophase and metaphase (SI Fig. 10*D*).

During mitosis, cells do not appear to internalize transferrin, a ligand specifically taken up by clathrin-coated vesicles (12, 13). These observations can be reconciled with our results, that clathrin-based endocytosis remains uniformly active during the cell cycle, if we recognize that significant reduction of recycling would greatly decrease the amount of transferrin receptor available on the cell surface. To test this hypothesis, we used established methods (18, 19) to measure the uptake of fluorescently labeled transferrin and to normalize that uptake to the number of accessible transferrin receptors with the potential to internalize ligand (SI Fig. 11). The amount of transferrin bound at the cell surface (Alexa488) or inside individual cells (Alexa594) was calculated from two-dimensional projections of three dimensional image stacks obtained by epifluorescence microscopy at different stages during the cell cycle (SI Fig. 11*A* for BSC1 cells and SI Fig. 11*B* for HeLa cells). We observed a substantial decrease in the amount of transferrin internalized during prophase and metaphase (Fig. 3, Internalized and SI Fig. 11), consistent with all previous observations. We further observed a marked decrease in the number of cell-surface receptors during prophase and metaphase followed by a very fast recovery starting with anaphase, and becoming very prominent with telophase and continuing into cytokinesis (Fig. 3 and SI Fig. 11, Surface), also in agreement with previous observations (13). The endocytic rate (18, 19), defined as the ratio of internalized transferrin to transferrin bound at the cell surface (In/Sur ratio), did not decrease during prophase and metaphase, but actually showed a modest but significant increase compared with the rate in cells during interphase or late stages of cytokinesis (Fig. 3). Previous measurements were not done in a way in which this ratio could have been measured in individual cells. Our results show that the reduction in transferrin internalization during mitosis does not correspond to an endocytic block, as formerly concluded, but instead that most of the receptors remain trapped within endosomes, most likely explained by a partial reduction in recycling rates, which are then released back to the cell surface as cytokinesis proceeds.

Recovery of the Plasma Membrane Correlates With Surface Bleb Formation. Live cell imaging, using phase contrast or fluorescence microscopy of adherent cells incubated with FM 1-43 throughout the recovery phase, shows the appearance of a large number of blebs at the outer surface of the cell, mostly at the distal poles and away from the cleavage furrow (SI Fig. 12 and SI Movies 5 and 6). These blebs appear and disappear rapidly (seconds) (SI Fig. 12*A*) until late stages of cytokinesis (SI Fig. 12*B*, 25 min). Bleb formation is not deleterious, because cells that have completed cytokinesis spread and remain viable (SI Fig. 12*B*, 52 min and SI Movie 6). Similar bebbling also occurs in confluent HeLa cells (SI Fig. 12*C* and SI Movie 7) and in the nonadherent human Jurkat T and insect Sf9 cells (SI Fig. 12 *D* and *E* and SI Movies 8 and 9).

Recovery of the Plasma Membrane Does Not Require a Functional Golgi Apparatus. The appearance of newly synthesized viral G protein at the cell surface is strongly inhibited during metaphase, anaphase, and early telophase (9). The images shown in SI Fig. 8*C* indicate a diffuse intracellular distribution of the Golgi marker, GalT-EGFP, during anaphase and telophase. Only during cytokinesis does this marker start to appear punctate and to localize in the perinuclear region (20, 21). Thus, a fully reorganized Golgi apparatus is not required for recovery of surface membrane. It is nonetheless possible that the substantial exocytic traffic in anaphase and telophase requires a functional postmitotic Golgi apparatus, even though a well localized GalT-EGFP perinuclear signal is still absent (20, 21). We ruled out involvement of a functional Golgi at this stage by observing the appearance of blebs during anaphase and telophase and during entrance to cytokinesis in cells treated with Brefeldin A before entering mitosis (SI Fig. 12*F* and SI Movie 10). The failure of Brefeldin A to prevent the rapid recovery of plasma membrane observed during anaphase and telophase shows that recovery can occur without the contribution of newly synthesized membranes from the Golgi. A similar Brefeldin A-insensitive membrane deposition at the cleavage furrow of sea urchin zygotes has been previously observed (22). However, a requirement for a

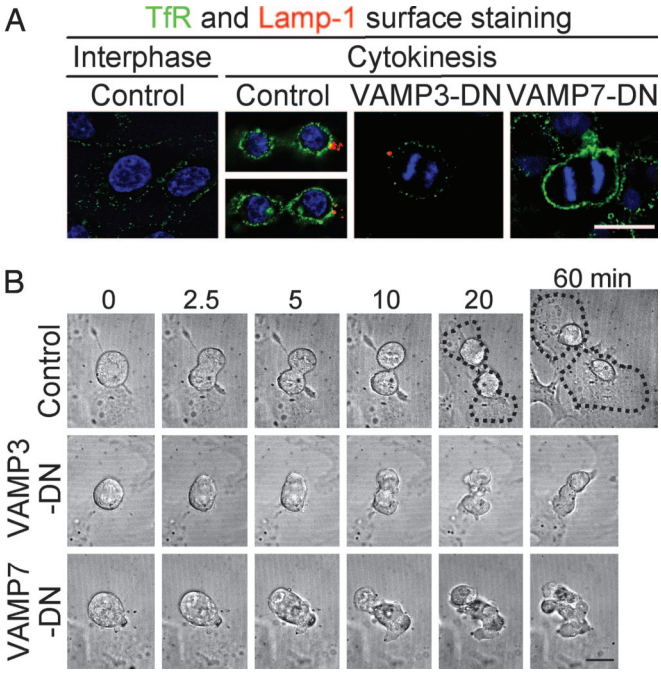

Fig. 4. Exocytosis is required during cell division. (*A*) Surface distribution of transferrin receptor and Lamp-1 during interphase and cytokinesis. HeLa cells were processed for immunofluorescence at 4°C by incubation with antibodies specific for the luminal domain of the transferrin receptor (green) and of Lamp-1 (red), followed by fixation and addition of fluorescently tagged secondary antibodies (Alexa-647 and Alexa-594, respectively). Images acquired in the absence (control) or presence of overexpressed cytosolic forms of the EGFP-labeled v-soluble N-ethylmaleimide-sensitive factor attachment protein receptors (V-SNAREs) (VAMP3-DN or VAMP7-DN). The cells expressing these constructs were identified by the cytosol EGFP signal (data not shown). The control panel (cytokinesis) corresponds to two optical sections 2 μm apart. Cells in interphase contain little Lamp-1 at their cell surface and stain weakly for transferrin receptor. Some blebs present during cytokinesis (control) score positive for Lamp-1, whereas others are labeled with transferrin receptor; the overall transferrin receptor signal is significantly stronger when compared with cells in interphase. Short expression (4–6 h) of VAMP3-DN prevents the surface expression of transferrin receptor but not of Lamp-1 in cells undergoing telophase; in contrast, similar expression of VAMP7-DN prevents the surface appearance of Lamp-1 but not of transferrin receptor. DNA was labeled with DAPI (blue). Scale bar, 20 μm. (*B*) Normal function of VAMP3 and VAMP7 is required for completion of cytokinesis. Top panel (control): Images acquired by bright field illumination of a BSC1 cell starting with anaphase, continuing through cytokinesis and ending with the spreading and separation of the two daughter cells. Middle panel (VAMP3-DN): images (from SI Movie 11) of BSC1 cell expressing VAMP3-DN for 4–6 h before imaging; blebs are present, ingression of the cleavage furrow occurs but cells do not separate. Bottom panel (VAMP7-DN): images (from SI Movie 12) of BSC1 cell expressing VAMP7-DN for 4–6 h before imaging; blebs are absent, ingression of the cleavage furrow occurs, but cells do not separate. Scale bar, 20 μm.

Brefeldin A-sensitive mechanism has been reported during membrane deposition at the apex of the late cleavage furrow in isolated, dividing *C. elegans* blastomeres (23) and during cell plate during plant cytokinesis (24).

Exocytosis Controls the Recovery of Plasma Membrane. Some of the blebs stain positively with an antibody specific for the luminal domain of Lamp-1, a marker of late endosomes and lysosomes normally absent from the cell surface during interphase (Fig. 4*A*, Interphase). Thus some blebs arise from fusion of Lamp-1 containing membranes with the plasma membrane (Fig. 4*A*, Cytokinesis, control). Other blebs are labeled with the internalized transferrin receptor (Fig. 4*A*, Cytokinesis, control), which accumulates even during mitosis in Lamp-1 negative early/recycling endosomes (SI Fig. 13). Still other blebs have neither Lamp-1 nor transferrin and may arise from additional endosomal compartments. Presumably these are the multilayer or single-membrane vesicles observed next to the blebs during late mitosis (6). Formation of these blebs seems to require the proper function of Myosin II, as their number was reduced in cells incubated during telophase with blebbistatin, an inhibitor of Myosin II (25) (SI Fig. 14*A*). Blebbistatin treatment also decreased the reappearance of internalized Lamp-1, but barely affected the recycling to the plasma membrane of transferrin receptor (SI Fig. 14*B*). These observations suggest that during cell division, the acto-myosin system has a role controlling fusion, particularly of late endosomes/lysosomes with the plasma membrane. They are consistent with the role of Myosin II in cell membrane repair as mediated by calcium-dependent exocytosis (26).

To further examine the relative contributions of early and late endosomes to plasma-membrane recovery, we took advantage of a published procedure (27, 28) to interfere with the fusion of either type of endosome to the plasma membrane. VAMP3-DN and VAMP7-DN are dominant negative cytosolic fragments of v-soluble N-ethylmaleimide-sensitive factor attachment protein receptors (V-SNAREs) specific for each path (27, 28). These fragments were transiently overexpressed for ≈4–6 h in BSC1 cells, and those cells entering mitosis were selected for imaging. We observed that expression of VAMP3-DN substantially decreased the reappearance of transferrin receptor (but not of Lamp-1) at the cell surface following anaphase (Fig. 4*A* and SI Fig. 15*A*); this interference coincided with an almost complete block in the recovery of plasma membrane (SI Fig. 15*B*) together with a failure to undergo cytokinesis (Fig. 4*B* and SI Movie 11). Expression for longer periods was not considered, because cell division was strongly inhibited and was accompanied by multiploidy in >80% of the cells (SI Fig. 15*C*). Likewise, short expression of the corresponding cytosolic fragment of VAMP7 prevented Lamp-1 reappearance (but not of transferrin receptor) at the cell surface (Fig. 4*A* and SI Fig. 15*A*), together with a significant block in plasma membrane recovery (SI Fig. 15*B*). Expression of VAMP7-DN also prevented cytokinesis (Fig. 4*B* and SI Movie 12) and induced mutliploidy (SI Fig. 15*D*). We conclude that both recycling and late endosomes participate in membrane redeposition.

Clathrin-Mediated Endocytosis Is Required for Retrieval of Plasma Membrane During Mitosis. Clathrin-mediated endocytosis is a high capacity membrane traffic pathway. It generally carries at least 50% of total endocytic traffic, and within 1 h it can internalize the equivalent of the entire cell surface (29). If, as proposed in *Endocytosis Is Not Affected During Mitosis*, endocytosis remains active during all stages of cell division, whereas exocytosis decreases substantially at the onset of mitosis, then reducing endocytosis during mitosis should prevent the decrease in cell surface and retard or prevent mitotic roundup. We confirmed this prediction in two ways. In one approach, we reduced clathrin-based endocytosis by depleting, with RNA interference in BSC1 (Fig. 5 and SI Fig. 16) or HeLa (SI Fig. 17) cells, the amount of μ2-adaptin, a component required to form the endocytic clathrin adaptor complex AP-2. As expected, 3 days of RNAi treatment was sufficient to block transferrin uptake (Fig. 5, Overlay). All cells with an equatorial disposition of chromosomes (metaphase) failed to round up; many (≈50%) had aberrant spindles (Fig. 5, DAPI and SI Fig. 16*A*, quantification). All remained flat and large, and their plasma membrane area was the same as control cells in interphase with normal endocytosis (SI Fig. 16*B*). This treatment also led to a significant accumulation of multinucleated cells because of incomplete cell division (SI Fig. 16*C*). In a second and complementary approach, we inhibited clathrin-

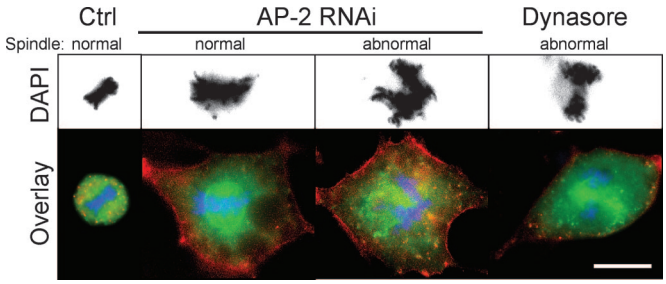

Fig. 5. Endocytosis is required for retrieval of plasma membrane during mitosis. BSC1 cells stably expressing EGFP-LCa were treated for 3 days with RNAi for μ2-adaptin to deplete AP-2 (center images) or for 30 min with 80 μM dynasore, a small molecule inhibitor of dynamin GTPase function (33) (rightmost image). These treatments inhibit clathrin-based endocytosis and during mitosis prevent cell rounding and loss of cell membrane (see SI Fig. 16*B*). Cells depleted of AP-2 and incubated for 5 min at 37°C with Alexa-594 transferrin (red) display surface staining, an almost complete absence of internalized transferrin, and the expected absence of endocytic clathrin coated pits and vesicles (EGFP-LCa, green). Because of the relative brief incubation with dynasore, these cells do not accumulate transferrin receptor at their surface even though receptor endocytosis is blocked; the punctate pattern of EGFP-LCa represents coated pits locked at the cell surface. A metaphase cell treated with only 0.8% DMSO (Ctrl) is shown. Whereas most control mitotic cells have normal spindles [decorated with EGFP-LCa, (53)], ≈50% of equivalent cells depleted of AP-2 or treated with dynasore display aberrant spindles (see SI Fig. 16*A*). Scale bar, 20 μm.

based endocytosis by acute interference with the function of dynamin, a large GTPase essential for coated vesicle formation (30–32). We incubated BSC1 cells for a brief interval with dynasore, a recently discovered small molecule inhibitor of the dynamin GTPase (33). Just as with the extended AP-2 depletion, 30 min incubation with 80 μM dynasore was sufficient to block transferrin uptake, to prevent cell rounding (Fig. 5), induce abnormal spindle formation (SI Fig. 16*A*), and decrease cell surface area (SI Fig. 16*B*); 0.8% DMSO, used as carrier, had no effect (Fig. 5).

Discussion

We have shown that the substantial decrease in total surface area that accompanies cell rounding is due mainly to a shutdown in membrane recycling from endosomal compartments back to the cell surface (Fig. 6). Most adherent cells in tissue culture round when they divide, and cells within tissues also acquire a spherical geometry during metaphase (34–37). This rounding appears to be important for ensuing proper spindle formation and appropriate distribution of components to the daughter cells and for establishing the correct intracellular spatial gradients for signaling molecules (38). Indeed, we find that failure to round up, induced by various forms of endocytic block, results in aberrant spindle formation and incorrect cell division.

We have also shown that plasma membrane recovery is essential for cell division. This rapid recovery is mediated by massive fusion of endosomal membranes, starting at the onset of anaphase and continuing through telophase. Our results provide a satisfying explanation for recent observations acquired in the course of RNAi screens aimed at identifying gene products important for cell division (39–42). Clathrin heavy chain, dynamin, Hsc70 (part of the uncoating machinery for the clathrin coat), a number of plasma membrane and Golgi-specific soluble N-ethylmaleimide-sensitive factor attachment protein receptors (SNAREs), subunits of the Golgi COPI complex, and regulatory small GTPases, such as Rab1 and Rab7, are among the proteins whose depletion have a clear impact in cell division.

The mechanisms that underlie membrane recovery studied here are probably distinct from a number of other processes in which new membrane is deposited. For example, specific structures such as the exocyst appear to participate in cleavage furrow formation and abscission at cytokinesis (43), and Golgi-derived vesicles are thought to contribute to the membranes laid down during cellularization in Drosophila (44) and endocytic vesicles (45). In plant cytokinesis, endocytic and Golgi-derived vesicles are the sources of material for phragmoplast deposition (46). In contrast, we propose here the formation of an internal membrane reservoir during rounding up which stores membrane components for subsequent release when called for later in cell division.

In addition to the experiments described here, we have also studied the potential role of Ca^{2+} in regulating exocytosis during mitosis (see *SI Results*). We suggest that Ca^{2+} signaling is essential for triggering the synchronous and coordinated fusion with the plasma membrane of endomembranes stored inside the cells, at a time when the Golgi apparatus has yet to assemble into a fully functional organelle. A rise in intracellular Ca^{2+} triggers rapid fusion of late endosomes and lysosomes with the plasma membrane (see ref. 47 for recent review); a similar process, also triggered by Ca^{2+}-influx during mechanical membrane injury, governs wound healing. Similarly, the Ca^{2+}-dependent membrane deposition required for the formation of a phagocytic cup (48, 49) derives, at least in part, from VAMP3 dependent recycling endosomes (27) and from VAMP7-dependent late endosomes (50). Perhaps the use of these pathways during cell division is the ancestral form. In contrast, normal traffic of recycling endosomes is not known to depend on Ca^{2+} signaling, at least during interphase.

It remains to be determined how modulation of these pathways occurs during mitosis. Control of these exocytic processes must be linked to stages in cell division, to produce endosomal recyling shutdown early in mitosis and to trigger abrupt reactivation at anaphase.

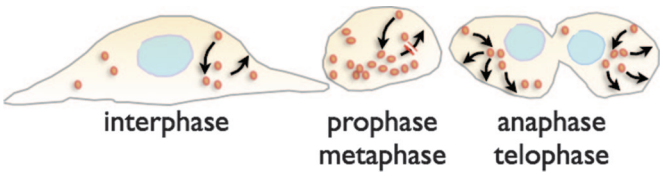

Fig. 6. Model for membrane traffic during different stages of the cell cycle. The schematic representations highlight the changes in balance of membrane traffic between endocytic routes and secretory together with recycling pathways during key stages of the cell cycle. These pathways are balanced during interphase. During the rounding up occurring during prophase and metaphase, the amount of plasma membrane decreases because of the traffic imbalance arising from normal endocytosis combined with a considerable decrease in secretory and recycling traffic, creating an internal ''membrane reservoir.'' During anaphase, telophase and cytokinesis the amount of plasma membrane increases rapidly along with the appearance of surface blebs. Most of the plasma membrane is recovered by the rapid fusion of the previously stored endo-membranes with the cell surface. A Ca^{2+} signal is required to trigger the rapid fusion of endomembranes with the plasma membrane in what constitutes a form of regulated exocytosis. At this stage, the Golgi apparatus is barely reassembled, and hence secretory traffic is still minimal.

Materials and Methods

Cell Preparation and Mitotic Stage Identification. The frequency of adherent cells undergoing mitosis was increased from ≈1% to 10–20% by allowing them to reach 100% confluency for 1 day, a condition where a large fraction of the cells are arrested at the end of G_1 (51). Cells were then trypsinized and seeded on 25-mm diameter glass no. 1.5 coverslips at ≈50–70% confluency; this plating condition increases significantly the proportion of cells simultaneously entering S phase at the time of seeding. Finally, cells were imaged 12–14 h (HeLa) or 18–20 h (BSC1) after

plating. Imaging by phase contrast bright field illumination was used to determine the stage of single cells along the cell cycle (selected from the unsynchronized population) according to the following criteria: cells in interphase appear flat, contain uncondensed chromosomes surrounded by a nuclear envelope; cells in prophase contain condensed chromosomes also surrounded by a nuclear envelope; cells in metaphase appear round, contain condensed chromosomes aligned at the metaphase plate and lack their nuclear envelope; cells in anaphase appear less round and contain two sets of condensed chromosomes each starting to migrate toward opposite spindle poles; cells in telophase start to develop the furrow or invagination separating the two daughter cells and still contain condensed chromosomes that reached the spindle poles; during cytokinesis, (imaged 20 min after the onset of anaphase), cells generate a deeper furrow, still display condensed chromosomes while the nuclear envelope starts to form around each chromosomal mass until abscission. All live cell imaging were performed as described in ref. 52 and *SI Methods*.

We thank Drs. A. Yu, S. Saffarian and R. Massol and the members of our laboratory for their help and advice, and Dr. J. Stow and J. Luzio for providing reagents. This work was supported by National Institutes of Health Grants GM075252 and GM62566 (to T.K.), by the Perkin Fund to purchase part of the imaging equipment used here, and the International Human Frontier Science Program Organization (to E.B.).

1. Meyers J, Craig J, Odde DJ (2006) *Curr Biol* 16:1685–1693.
2. Ohnuma K, Yomo T, Asashima M, Kaneko K (2006) *Bioorg Med Chem Cell Biol* 7:25.
3. Knutton S, Sumner MC, Pasternak CA (1975) *J Cell Biol* 66:568–576.
4. Erickson CA, Trinkaus JP (1976) *Exp Cell Res* 99:375–384.
5. Porter K, Prescott D, Frye J (1973) *J Cell Biol* 57:815–836.
6. Bluemink JG, van Maurik PA, Tertoolen LG, van der Saag PT, de Laat SW (1983) *Eur J Cell Biol* 32:7–16.
7. Albertson R, Riggs B, Sullivan W (2005) *Trends Cell Biol* 15:92–101.
8. Lucocq JM, Warren G (1987) *EMBO J* 6:3239–3246.
9. Warren G, Featherstone C, Griffiths G, Burke B (1983) *J Cell Biol* 97:1623–1628.
10. Berlin RD, Oliver JM, Walter RJ (1978) *Cell* 15:327–341.
11. Berlin RD, Oliver JM (1980) *J Cell Biol* 85:660–671.
12. Sager PR, Brown PA, Berlin RD (1984) *Cell* 39:275–282.
13. Warren G, Davoust J, Cockcroft A (1984) *EMBO J* 3:2217–2225.
14. Schweitzer JK, Burke EE, Goodson HV, D'Souza-Schorey C (2005) *J Biol Chem* 280:41628–41635.
15. Brumback AC, Lieber JL, Angleson JK, Betz WJ (2004) *Methods* 33:287–294.
16. Pypaert M, Lucocq JM, Warren G (1987) *Eur J Cell Biol* 45:23–29.
17. Ehrlich M, Boll W, Van Oijen A, Hariharan R, Chandran K, Nibert ML, Kirchhausen T (2004) *Cell* 118:591–605.
18. Wiley HS, Cunningham DD (1982) *J Biol Chem* 257:4222–4229.
19. Ghosh RN, Gelman DL, Maxfield FR (1994) *J Cell Sci* 107(8):2177–2189.
20. Souter E, Pypaert M, Warren G (1993) *J Cell Biol* 122:533–540.
21. Jiang S, Rhee SW, Gleeson PA, Storrie B (2006) *Mol Biol Cell* 17:4105–4117.
22. Shuster CB, Burgess DR (2002) *Proc Natl Acad Sci USA* 99:3633–3638.
23. Skop AR, Bergmann D, Mohler WA, White JG (2001) *Curr Biol* 11:735–746.
24. Yasuhara H, Sonobe S, Shibaoka H (1995) *Eur J Cell Biol* 66:274–281.
25. Straight AF, Cheung A, Limouze J, Chen I, Westwood NJ, Sellers JR, Mitchison TJ (2003) *Science* 299:1743–1747.
26. Togo T, Steinhardt RA (2004) *Mol Biol Cell* 15:688–695.
27. Murray RZ, Kay JG, Sangermani DG, Stow JL (2005) *Science* 310:1492–1495.
28. Martinez-Arca S, Alberts P, Zahraoui A, Louvard D, Galli T (2000) *J Cell Biol* 149:889–900.
29. Hansen SH, Sandvig K, van Deurs B (1992) *Exp Cell Res* 199:19–28.
30. Praefcke GJ, McMahon HT, Engqvist-Goldstein AE, Drubin DG, Lang T, Korolchuk V, Banting G, Song BD, Schmid SL, Wiejak J, *et al.* (2004) *Nat Rev Mol Cell Biol* 5:133–147.
31. Schmid SL, McNiven MA, De Camilli P (1998) *Curr Opin Cell Biol* 10:504–512.
32. McNiven MA (1998) *Cell* 94:151–154.
33. Macia E, Ehrlich M, Massol R, Boucrot E, Brunner C, Kirchhausen T (2006) *Dev Cell* 10:839–850.
34. Seery JP, Watt FM (2000) *Curr Biol* 10:1447–1450.
35. Gong Y, Mo C, Fraser SE (2004) *Nature* 430:689–693.
36. Lechler T, Fuchs E (2005) *Nature* 437:275–280.
37. Gibson MC, Patel AB, Nagpal R, Perrimon N (2006) *Nature* 442:1038–1041.
38. Bastiaens P, Caudron M, Niethammer P, Karsenti E (2006) *Trends Cell Biol* 16:125–134.
39. Kiger AA, Baum B, Jones S, Jones MR, Coulson A, Echeverri C, Perrimon N (2003) *J Biol* 2:27.
40. Eggert US, Kiger AA, Richter C, Perlman ZE, Perrimon N, Mitchison TJ, Field CM (2004) *PLoS Biol* 2:e379.
41. Echard A, Hickson GR, Foley E, O'Farrell PH (2004) *Curr Biol* 14:1685–1693.
42. Bjorklund M, Taipale M, Varjosalo M, Saharinen J, Lahdenpera J, Taipale J (2006) *Nature* 439:1009–1013.
43. Gromley A, Yeaman C, Rosa J, Redick S, Chen CT, Mirabelle S, Guha M, Sillibourne J, Doxsey SJ (2005) *Cell* 123:75–87.
44. Papoulas O, Hays TS, Sisson JC (2005) *Nat Cell Biol* 7:612–618.
45. Lecuit T, Wieschaus E (2000) *J Cell Biol* 150:849–860.
46. Dhonukshe P, Baluska F, Schlicht M, Hlavacka A, Samaj J, Friml J, Gadella TW, Jr (2006) *Dev Cell* 10:137–150.
47. McNeil PL, Kirchhausen T (2005) *Nat Rev Mol Cell Biol* 6:499–505.
48. Tapper H, Furuya W, Grinstein S (2002) *J Immunol* 168:5287–5296.
49. Czibener C, Sherer NM, Becker SM, Pypaert M, Hui E, Chapman ER, Mothes W, Andrews NW (2006) *J Cell Biol* 174:997–1007.
50. Braun V, Fraisier V, Raposo G, Hurbain I, Sibarita JB, Chavrier P, Galli T, Niedergang F (2004) *EMBO J* 23:4166–4176.
51. Coupin GT, Muller CD, Remy-Kristensen A, Kuhry JG (1999) *J Cell Sci* 112(14):2431–2440.
52. Massol RH, Boll W, Griffin AM, Kirchhausen T (2006) *Proc Natl Acad Sci USA* 103:10265–10270.
53. Royle SJ, Bright NA, Lagnado L (2005) *Nature* 434:1152–1157.